Bassham (CBB) pathway but fixes CO_2 and contributes to adenosine monophosphate (AMP) recycling (*7*, *24*). We predict that the bacterial type II/III RuBisCO genes share this function. Homologs of DeoA and E2b2, key enzymes of the CO_2-fixing AMP-recycling pathway (*24*), were identified (Fig. 3B), and no essential CBB cycle enzymes (e.g., phosphoribulokinase) were detected. Salvaging purine-pyrimidine products to produce RuBisCO generates 3-phosphoglycerates and perhaps pyruvate (ACD80), which could ultimately be fermented for ATP production (*7*).

From this study and rRNA gene survey information indicating prevalence in anoxic, organic carbon-rich environments (*25*, *26*), we predict widespread fermentation-based metabolism in the 49 OD1, OP11, BD1-5, and PER genomes sampled here. We find it intriguing that several pathways for anoxic carbon, hydrogen, and sulfur cycling in these organisms share features previously documented only in Archaea. Some OD1 may contribute to sulfur cycling, on the basis of their previous association with sulfur-rich environments (*11*, *12*, *26*–*28*). Given the absence of genes for sulfur respiration in our near-complete OD1-i genomes, the link may involve hydrogenase-mediated sulfur-reductase activity. Notably, these insights were obtained through cultivation-independent analyses and have contributed more near-complete (>90%) genomic sampling for OD1 than is available for almost half of all of the genomically characterized bacterial phyla (*29*).

References and Notes

1. M. Hess *et al.*, *Science* **331**, 463 (2011).
2. D. Wu *et al.*, *PLoS ONE* **6**, e18011 (2011).
3. G. W. Tyson *et al.*, *Nature* **428**, 37 (2004).
4. V. Iverson *et al.*, *Science* **335**, 587 (2012).
5. P. G. Falkowski, T. Fenchel, E. F. Delong, *Science* **320**, 1034 (2008).
6. M. S. Rappé, S. J. Giovannoni, *Annu. Rev. Microbiol.* **57**, 369 (2003).
7. Materials and methods are available as supplementary materials on *Science* Online.
8. C. S. Miller, B. J. Baker, B. C. Thomas, S. W. Singer, J. F. Banfield, *Genome Biol.* **12**, R44 (2011).
9. G. J. Dick *et al.*, *Genome Biol.* **10**, R85 (2009).
10. J. Raes, J. O. Korbel, M. J. Lercher, C. von Mering, P. Bork, *Genome Biol.* **8**, R10 (2007).
11. M. S. Elshahed *et al.*, *Appl. Environ. Microbiol.* **71**, 7598 (2005).
12. N. H. Youssef, P. C. Blainey, S. R. Quake, M. S. Elshahed, *Appl. Environ. Microbiol.* **77**, 7804 (2011).
13. J. P. McCutcheon, B. R. McDonald, N. A. Moran, *PLoS Genet.* **5**, e1000565 (2009).
14. X. Mai, M. W. Adams, *J. Bacteriol.* **178**, 5897 (1996).
15. R. T. Anderson *et al.*, *Appl. Environ. Microbiol.* **69**, 5884 (2003).
16. L. Schöcke, B. Schink, *Eur. J. Biochem.* **256**, 589 (1998).
17. P. M. Vignais, B. Billoud, *Chem. Rev.* **107**, 4206 (2007).
18. K. Ma, R. N. Schicho, R. M. Kelly, M. W. Adams, *Proc. Natl. Acad. Sci. U.S.A.* **90**, 5341 (1993).
19. D. J. van Haaster, P. J. Silva, P. L. Hagedoorn, J. A. Jongejan, W. R. Hagen, *J. Bacteriol.* **190**, 1584 (2008).
20. R. Sapra, K. Bagramyan, M. W. W. Adams, *Proc. Natl. Acad. Sci. U.S.A.* **100**, 7545 (2003).
21. P. J. Silva *et al.*, *Eur. J. Biochem.* **267**, 6541 (2000).
22. T. Kanai *et al.*, *J. Bacteriol.* **193**, 3109 (2011).
23. F. R. Tabita, T. E. Hanson, S. Satagopan, B. H. Witte, N. E. Kreel, *Philos. Trans. R. Soc. B* **363**, 2629 (2008).
24. T. Sato, H. Atomi, T. Imanaka, *Science* **315**, 1003 (2007).
25. C. Briée, D. Moreira, P. López-García, *Res. Microbiol.* **158**, 213 (2007).
26. S. Peura *et al.*, *ISME J.* **6**, 1640 (2012).
27. P. Hugenholtz, C. Pitulle, K. L. Hershberger, N. R. Pace, *J. Bacteriol.* **180**, 366 (1998).
28. J. K. Harris, S. T. Kelley, N. R. Pace, *Appl. Environ. Microbiol.* **70**, 845 (2004).
29. I. Pagani *et al*, *Nucleic Acids Res.* **40** (Database issue), D571 (2012).

Acknowledgments: We thank F. Larimer for RuBisCO analyses input; M. Shah for proteomic support; C. Thrash, P. Hugenholtz, and J. Eisen for manuscript suggestions; and the U.S. Department of Energy (DOE) Subsurface Biogeochemistry Program for funding, the DOE Knowledgebase Program for funding GGkbase, and EMBO for a fellowship to I.S. The Rifle, Colorado, Integrated Field Research Center Project is managed by Lawrence Berkeley National Laboratory for the U.S. DOE (contract no. DE-AC02-05CH11231). Portions of this work were performed in the Environmental Molecular Science Laboratory, a DOE national scientific user facility at Pacific Northwest National Laboratory. The sequences were deposited in the National Center for Biotechnology Information Sequence Read Archive (accession no. SRA050978.1). This Whole-Genome Shotgun project has been deposited at GenBank under the accession no. AMFJ00000000. The version described in this paper is the first version, AMFJ01000000. Genomic and proteomic data can be accessed via http://geomicrobiology.berkeley.edu/rifle/acd_ggkbase.html.

Supplementary Materials

www.sciencemag.org/cgi/content/full/337/6102/1661/DC1
Materials and Methods
Supplementary Text
Figs. S1 to S9
Tables S1 to S6
References (*30*–*58*)
Database 1

3 April 2012; accepted 18 July 2012
10.1126/science.1224041

Disulfide Rearrangement Triggered by Translocon Assembly Controls Lipopolysaccharide Export

Shu-Sin Chng,[1,2]*† Mingyu Xue,[1]† Ronald A. Garner,[1] Hiroshi Kadokura,[2,3] Dana Boyd,[2] Jonathan Beckwith,[2] Daniel Kahne[1,4]‡

The presence of lipopolysaccharide (LPS) on the cell surface of Gram-negative bacteria is critical for viability. A conserved β-barrel membrane protein LptD (lipopolysaccharide transport protein D) translocates LPS from the periplasm across the outer membrane (OM). In *Escherichia coli*, this protein contains two disulfide bonds and forms the OM LPS translocon with the lipoprotein LptE. Here, we identified seven in vivo states on the oxidative-folding pathway of LptD. Proper assembly involved a nonfunctional intermediate containing non-native disulfides. Intermediate formation required the oxidase DsbA, and subsequent maturation to the active form with native disulfides was triggered by LptE. Thus, disulfide bond–dependent protein folding of LptD requires the proper assembly of a two-protein complex to promote disulfide bond rearrangement.

A defining feature of Gram-negative organisms is the presence of lipopolysaccharide (LPS) on the cell surface (*1*). LPS must be properly assembled in the outer leaflet of the outer membrane (OM) to establish a permeability barrier against toxic compounds, including antibiotics (*2*, *3*). In *Escherichia coli*, a translocon responsible for LPS movement across the OM is composed of two essential OM proteins: an integral β-barrel protein, LptD (lipopolysaccharide transport protein D), and a lipoprotein, LptE (*4*–*6*). The LptD/E complex forms part of the trans-envelope LPS exporter, which contains five other essential Lpt proteins that collectively move LPS from the inner membrane (IM) to the cell surface (*7*). Assembly of the OM LPS translocon presents a challenging protein-folding problem, because LptE resides inside LptD (*5*, *6*) and formation of the correct disulfide bonds in LptD is required for this translocon to function (*8*). How the cell coordinates assembly of the OM complex with the formation of the rest of the trans-envelope exporter is unknown.

To understand the assembly of the functional OM LPS translocon, we examined the biogenesis of LptD. *E. coli* LptD contains an N-terminal periplasmic domain (amino acids 25 to 202) and a C-terminal integral β-barrel domain (amino acids 203 to 784) (*5*), which is folded and inserted into the OM by the Bam complex (β-barrel assembly machine) (*9*–*11*). LptD has four cysteine residues, two in the N-terminal domain (Cys^{31} and Cys^{173}) and two very near the C terminus (Cys^{724} and Cys^{725}). In its mature form, LptD contains two long-range nonconsecutive disulfide bonds connecting the N- and C-terminal domains, one

[1]Department of Chemistry and Chemical Biology, Harvard University, Cambridge, MA 02138, USA. [2]Department of Microbiology and Immunobiology, Harvard Medical School, Boston, MA 02115, USA. [3]Graduate School of Biological Sciences, Nara Institute of Science and Technology, 8916-5, Takayama, Ikoma, Nara 630-0192, Japan. [4]Department of Biological Chemistry and Molecular Pharmacology, Harvard Medical School, Boston, MA 02115, USA.

*Present address: Department of Chemistry, National University of Singapore, Singapore 117543.
†These authors contributed equally to this work.
‡To whom correspondence should be addressed. E-mail: kahne@chemistry.harvard.edu

between the first and third cysteines (Cys^{31}-Cys^{724}; [**1-3**]) and the other between the second and fourth cysteines (Cys^{173}-Cys^{725}; [**2-4**]) (Fig. 1A) (*8*). Either of these two disulfides is sufficient for LptD to function (*8*).

LptE is required to promote assembly of mature LptD (*8*). We wondered if an LptD intermediate would accumulate in vivo when LptE is the limiting reagent. OM fragments isolated from wild-type (WT) cells contain only mature LptD, which migrates more slowly than reduced LptD during SDS–polyacrylamide gel electrophoresis (PAGE) (Fig. 1A) (*8*, *12*, *13*). In contrast, OM fragments from an LptE-limiting strain, which produced lower levels of LptE (fig. S1), contained a new LptD species. In the absence of β-mercaptoethanol, this species migrated slightly faster than fully reduced LptD, suggesting that it was disulfide-bonded (Fig. 1A). To assign the disulfide connectivity of this LptD species (intermediate **1**), we examined the SDS-PAGE migration patterns of the six LptD mutant proteins in which two of the cysteines were changed to serine residues (*8*). Only the mutant lacking the last two cysteines ($LptD_{CCSS}$), which can make the Cys^{31}-Cys^{173} ([**1-2**]) disulfide bond within the N-terminal domain, exhibited faster mobility than reduced LptD (fig. S2). Thus, the LptD intermediate **1** that accumulates when LptE is limiting contains the consecutive [**1-2**] disulfide bond, and LptE is required for the conversion of this intermediate to LptD with its native disulfide bonds. Whether the third and fourth cysteines are ever disulfide-bonded in this intermediate remains unclear, although we have obtained some evidence suggesting that the [**3-4**] disulfide bond may be formed (fig. S3).

To examine how defects in either component affect translocon assembly, we analyzed three mutants: $LptD_{\Delta 330\text{-}352}$ (LptD4213) (*14*), $LptD_{\Delta 529\text{-}538}$ (*6*), and $LptE_{\Delta 100\text{-}101/P99R}$ (LptE6) (*15*). Two of these mutations impair interactions between LptD and LptE (*6*, *15*). Although none of these mutations lowered the levels of LptE in the OM, each resulted in substantial accumulation of intermediate **1** ([**1-2**]–LptD) (Fig. 1B). LptD containing a [**1-2**] disulfide bond is not functional (*8*), which explains why these mutants have defective OMs (*6*, *14*, *15*).

To determine whether intermediate **1** is a dead-end product or on the folding pathway of LptD in a WT strain, we pulse-labeled $FLAG_3$-tagged LptD with [^{35}S]-methionine and monitored its progression to the mature form during a cold-methionine chase. The predominant form at the start of the chase was [**1-2**]–LptD (intermediate **1**), which was slowly converted to mature [**1-3**][**2-4**]–LptD (Fig. 2A). The final distribution of LptD species at ~20 min was identical to that in the steady state (fig. S4, A and B). Thus, a non-native species with a disulfide bond (intermediate **1**) is an intermediate along the oxidative-folding pathway of LptD in vivo. Furthermore, formation of mature [**1-3**][**2-4**]–LptD proceeds via disulfide bond rearrangement.

We next performed pulse-chase experiments under conditions that preserve a folded β barrel to determine whether disulfide bond rearrangement occurs before or after β-barrel folding. When samples were not heated before SDS-PAGE, mature [**1-3**][**2-4**]–LptD migrated as a broad band with faster gel mobility than the heat-denatured form, indicating that the β barrel was folded (Fig. 2B) (*5*). The amount of folded [**1-3**][**2-4**]–LptD increased with time. A new, fast-migrating LptD species, appearing at the start and chasing away by 20 min, could be detected (Fig. 2B). This species was also heat-modifiable and ran at the same position as the major band in a nonheated $LptD_{CCSS}$ sample containing the [**1-2**] disulfide (Fig. 2B). We assign this LptD species as intermediate **1** containing a folded β barrel. Because folded intermediate **1** chased to folded mature [**1-3**][**2-4**]–LptD, we conclude that the LptD β barrel folds before disulfide rearrangement occurs. Furthermore, monitoring protease susceptibility supported this notion (fig. S5). Because this [**1-2**]–LptD species did not accumulate substantially during the chase, we conclude that folding is slower than rearrangement.

LptD is a substrate of the periplasmic oxidase DsbA (*16*), and oxidation of LptD is impaired in strains lacking DsbA (fig. S4) (*8*, *12*). We sought to elucidate the role of DsbA in introducing disulfide bonds in LptD by using the $DsbA_{P151T}$ mutant that forms kinetically stable mixed-disulfide intermediates with substrate proteins to see if we could accumulate cross-linked adducts between LptD and DsbA (*16*). We observed two LptD species that also contained

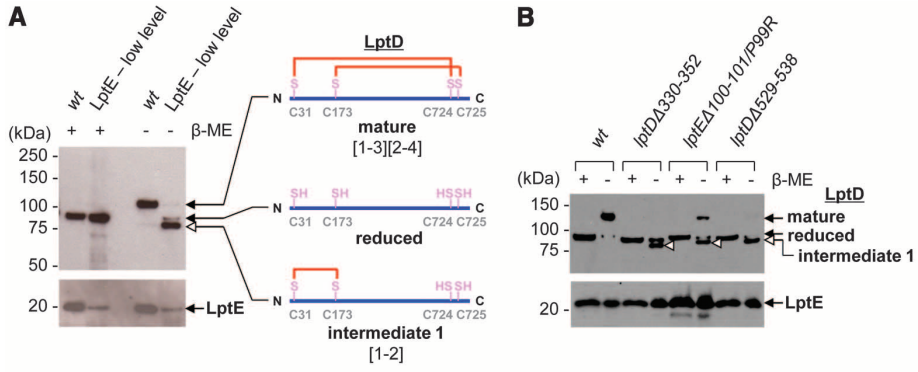

Fig. 1. A non-native LptD intermediate with a disulfide bond (**1**, [**1-2**]–LptD) accumulates in strains with defective LptD or LptE. (**A**) α-LptD and α-LptE immunoblot analyses of OM fragments obtained from wild-type (*wt*) and LptE-limiting strains grown to early log phase (see fig. S1). More membranes (3×) from cells expressing limited LptE were loaded. (**B**) α-LptD and α-LptE immunoblot analyses of OM fragments obtained from *wt*, $lptD_{\Delta 330\text{-}352}$, $lptE_{\Delta 100\text{-}101/P99R}$, and $lptD_{\Delta 529\text{-}538}$ strains. White arrowheads indicate the position of [**1-2**]–LptD in each strain. Where indicated, β-mercaptoethanol (β-ME) was used to reduce disulfide bonds.

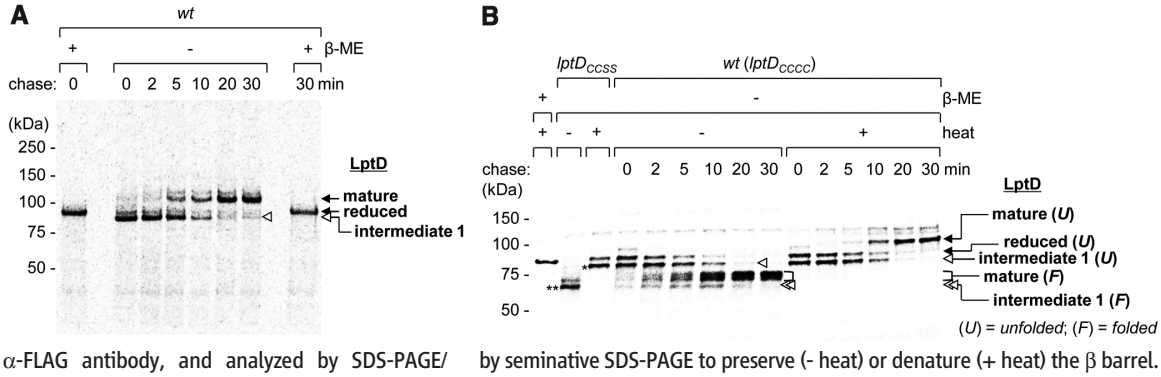

Fig. 2. Intermediate **1** is observed along the LptD assembly pathway in vivo. Folding of the LptD β-barrel domain is slow and precedes disulfide bond rearrangement. (**A**) WT cells expressing LptD-$FLAG_3$ were pulsed with [^{35}S]-methionine and chased with cold methionine. The samples were alkylated with *N*-ethylmaleimide, immunoprecipitated with α-FLAG antibody, and analyzed by SDS-PAGE/autoradiography. (**B**) [^{35}S]-Met pulse-chase of newly synthesized LptD-$FLAG_3$, where samples were processed under nondenaturing conditions and analyzed by seminative SDS-PAGE to preserve (- heat) or denature (+ heat) the β barrel. Pulse-labeled $LptD_{CCSS}$-$FLAG_3$ marks the positions of unfolded (single asterisk) and folded (double asterisks) [**1-2**]–LptD.

DsbA (Fig. 3A). We then identified these new bands as mixed-disulfide intermediates linking DsbA to Cys^{31} of reduced LptD (DsbA adduct **A**; [**1**-**DsbA**]) and to Cys^{31} of [**2**-**4**]–LptD (DsbA adduct **B**; [**2**-**4**][**1**-**DsbA**]) by comparing adducts observed with LptD using Cys-to-Ser mutants (Fig. 3, A and C, and fig. S6). DsbA adduct **A** was likely to correspond to the intermediate that first formed between LptD and DsbA, leading to the formation of the [**1**-**2**] disulfide bond (Fig. 3C). When we performed pulse-chase analysis in the *dsbA*$_{P151T}$ strain, we detected [^{35}S]-labeled DsbA adduct **A** at early time points (t = 0 to 2 min) (Fig. 3B), consistent with this interpretation. We also observed the appearance of DsbA adduct **B** ([**2**-**4**][**1**-**DsbA**]–LptD) at t = 2 min, which chased by t = 40 min. The fact that this species appeared before (and chased into) [**1**-**3**][**2**-**4**]–LptD suggests that DsbA adduct **B** is also along the assembly pathway and that DsbA directly introduces the [**1**-**3**] disulfide bond in LptD after an intermediate containing the [**2**-**4**] disulfide bond (intermediate **2**, see fig. S4) is already formed (Fig. 3C). Thus, DsbA makes both the [**1**-**2**] and [**1**-**3**] disulfide bonds in LptD at different stages of assembly.

The ability to detect several DsbA adducts with LptD during pulse-chase analysis allowed us to describe the sequence of events leading to the assembly of a functional OM LPS translocon. We could assign seven distinct species along the oxidative-folding pathway of LptD in vivo (Fig. 3C). The first nonconsecutive disulfide bond formed between Cys^{173} and Cys^{725} ([**2**-**4**]) via disulfide bond rearrangement from [**1**-**2**]–LptD. Because either of the two nonconsecutive disulfide bonds is sufficient for the proper function of LptD (*8*), the [**2**-**4**]–LptD species (intermediate **2**) represents the first functional form of LptD. In this regard, it is important to point out that both Cys^{173} and Cys^{725} are present in >95% of more than 1000 Gram-negative LptD proteins that have nonidentical sequences (fig. S7) (*12*). In contrast, Cys^{31} and Cys^{724} are much less conserved, suggesting that the [**2**-**4**] disulfide bond plays a critical structural role in the function of the translocon.

LptD and LptE function together in a single step to insert LPS correctly on the cell surface (*4*–*6*). The progression of LptD from an unfolded intermediate to a preassembled nonfunctional complex with LptE containing non-native disulfide bonds (intermediate **1**), and then to a rearranged functional state containing native disulfide bonds, provides a mechanism to check that both translocon components have been properly synthesized, targeted, and assembled together in the OM. Mutants in LptD or LptE accumulate intermediate **1** (Fig. 1B), suggesting that assembly of the translocon stalls in a nonfunctional state if there are defects in either component. Intermediate **1** also accumulates in strains with limited LptE (Fig. 1A), but it can be completely converted to the functional form of LptD if additional LptE is subsequently expressed (fig. S8). This "rescue" experiment demonstrates that increased LptE levels, which permit formation of the plug-and-barrel architecture, trigger rearrangement of the disulfide bonds. Thus, assembly of the LptD/E complex controls activation of the translocon; only when the complex is properly formed does disulfide bond rearrangement occur efficiently (Fig. 3C). The oxidative assembly of LptD is regulated by disulfide bond rearrangement that is triggered by binding to LptE, which, in fact, is not even an oxidoreductase.

Producing nonfunctional intermediate **1** before activation via disulfide bond rearrangement also provides a mechanism for quality control to ensure that the trans-envelope LPS exporter is assembled with only a functional OM translocon (Fig. 3C). Proper disulfide bonds in LptD are required for the trans-envelope Lpt bridge to form via interactions between LptA and LptD (*17*). The triggering strategy prevents a defective OM translocon from achieving the correct disulfide bond configuration, thereby preventing formation of a nonfunctional trans-envelope LPS exporter that might release LPS into an inappropriate compartment.

Our ability to visualize and accumulate different oxidation states of LptD allows us to extend

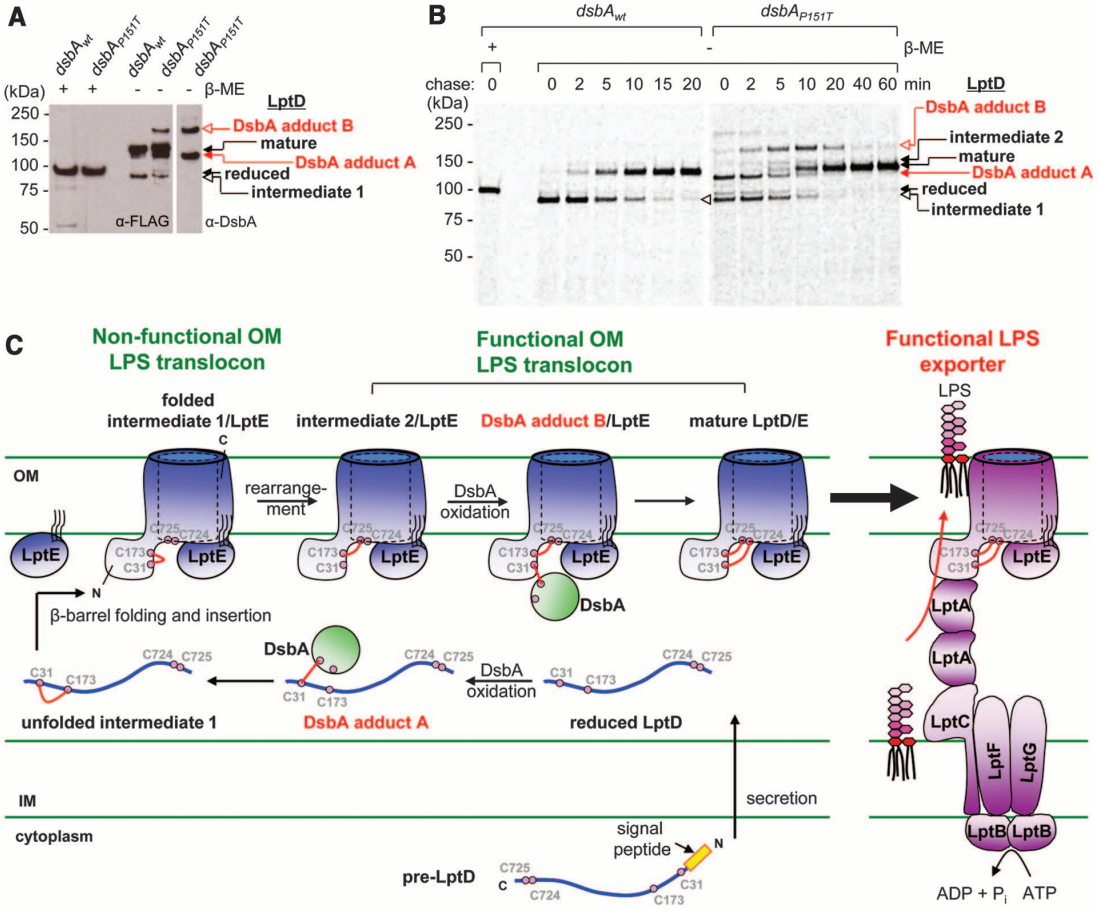

Fig. 3. The oxidative-folding pathway of LptD. (**A**) LptD intermediates containing mixed-disulfide adducts with DsbA can be detected in vivo. α-FLAG immunoprecipitation using *wt* or *dsbA*$_{P151T}$ cells containing pET23/42*lptD-FLAG*$_3$. Samples were analyzed by α-FLAG and α-DsbA immunoblots. (**B**) [^{35}S]-Met pulse-chase of newly synthesized LptD-FLAG$_3$ in *wt* and *dsbA*$_{P151T}$ backgrounds. (**C**) Biogenesis of the trans-envelope LPS exporter. The six intermediate LptD species observed experimentally are depicted as they appear after secretion across the IM during oxidative assembly of the OM translocon. ADP, adenosine diphosphate; P_i, inorganic phosphate; ATP, adenosine triphosphate.

to membrane proteins the classic approach of using disulfide bonds to study the folding of soluble proteins in vivo (*18*, *19*). Our studies have established that the rate-determining step in translocon assembly is β-barrel folding. Folding is remarkably slow, taking ~20 min, or one-third of the cell cycle (Fig. 2). The porin LamB folds several orders of magnitude faster than LptD (*20*). LptD folding may be slow because the protein must wrap around LptE, forming a β barrel that also contains a plug (*5*, *6*). Given the slow rate of LptD folding, it may be possible to design inhibitors against the long-lived nonfunctional states of the OM LPS translocon, thus preventing its activation.

References and Notes

1. C. R. H. Raetz, C. Whitfield, *Annu. Rev. Biochem.* **71**, 635 (2002).
2. P. F. Mühlradt, J. R. Golecki, *Eur. J. Biochem.* **51**, 343 (1975).
3. H. Nikaido, *Microbiol. Mol. Biol. Rev.* **67**, 593 (2003).
4. T. Wu *et al.*, *Proc. Natl. Acad. Sci. U.S.A.* **103**, 11754 (2006).
5. S. S. Chng, N. Ruiz, G. Chimalakonda, T. J. Silhavy, D. Kahne, *Proc. Natl. Acad. Sci. U.S.A.* **107**, 5363 (2010).
6. E. Freinkman, S. S. Chng, D. Kahne, *Proc. Natl. Acad. Sci. U.S.A.* **108**, 2486 (2011).
7. S. S. Chng, L. S. Gronenberg, D. Kahne, *Biochemistry* **49**, 4565 (2010).
8. N. Ruiz, S. S. Chng, A. Hiniker, D. Kahne, T. J. Silhavy, *Proc. Natl. Acad. Sci. U.S.A.* **107**, 12245 (2010).
9. U. S. Eggert *et al.*, *Science* **294**, 361 (2001).
10. T. Wu *et al.*, *Cell* **121**, 235 (2005).
11. J. G. Sklar *et al.*, *Proc. Natl. Acad. Sci. U.S.A.* **104**, 6400 (2007).
12. M. Braun, T. J. Silhavy, *Mol. Microbiol.* **45**, 1289 (2002).
13. Materials and methods are available as supplementary materials on *Science* Online.
14. B. A. Sampson, R. Misra, S. A. Benson, *Genetics* **122**, 491 (1989).
15. G. Chimalakonda *et al.*, *Proc. Natl. Acad. Sci. U.S.A.* **108**, 2492 (2011).
16. H. Kadokura, H. Tian, T. Zander, J. C. A. Bardwell, J. Beckwith, *Science* **303**, 534 (2004).
17. E. Freinkman, S. Okuda, N. Ruiz, D. Kahne, *Biochemistry* **51**, 4800 (2012).
18. H. Kadokura, J. Beckwith, *Cell* **138**, 1164 (2009).
19. A. Jansens, E. van Duijn, I. Braakman, *Science* **298**, 2401 (2002).
20. A. R. Ureta, R. G. Endres, N. S. Wingreen, T. J. Silhavy, *J. Bacteriol.* **189**, 446 (2007).

Acknowledgments: We thank E. Freinkman for pET23/42*lptD-FLAG*$_3$. J.B. is an American Cancer Society Professor. This work is supported by NIH grants AI081059 (to D.K.) and NIGMS 41883 (to J.B.) and in part by Japan Society for the Promotion of Science Grant-in-Aid for Scientific Research (C) 21580092 (to H.K.).

Supplementary Materials

www.sciencemag.org/cgi/content/full/science.1227215/DC1
Materials and Methods
Figs. S1 to S8
References (*21*, *22*)

2 May 2012; accepted 3 August 2012
Published online 30 August 2012;
10.1126/science.1227215

Sedlin Controls the ER Export of Procollagen by Regulating the Sar1 Cycle

Rossella Venditti,[1]* Tiziana Scanu,[2]*† Michele Santoro,[1] Giuseppe Di Tullio,[2] Alexander Spaar,[2] Renato Gaibisso,[2] Galina V. Beznoussenko,[2]‡ Alexander A. Mironov,[2]‡ Alexander Mironov Jr.,[2]§ Leopoldo Zelante,[3] Maria Rosaria Piemontese,[3] Angelo Notarangelo,[3] Vivek Malhotra,[4,5] Barbara M. Vertel,[6] Cathal Wilson,[1] Maria Antonietta De Matteis[1]||

Newly synthesized proteins exit the endoplasmic reticulum (ER) via coat protein complex II (COPII) vesicles. Procollagen (PC), however, forms prefibrils that are too large to fit into typical COPII vesicles; PC thus needs large transport carriers, which we term megacarriers. TANGO1 assists PC packing, but its role in promoting the growth of megacarriers is not known. We found that TANGO1 recruited Sedlin, a TRAPP component that is defective in spondyloepiphyseal dysplasia tarda (SEDT), and that Sedlin was required for the ER export of PC. Sedlin bound and promoted efficient cycling of Sar1, a guanosine triphosphatase that can constrict membranes, and thus allowed nascent carriers to grow and incorporate PC prefibrils. This joint action of TANGO1 and Sedlin sustained the ER export of PC, and its derangement may explain the defective chondrogenesis underlying SEDT.

Newly synthesized protein cargoes are exported from the endoplasmic reticulum (ER) in transport carriers. Cargo sorting and carrier budding occur at ER exit sites (ERES) and are mediated by the small guanosine triphosphatase (GTPase) Sar1, which recruits the COPII coat complex (*1*). Procollagen (PC), however, forms 300-nm triple helices whose size exceeds that of typical 60- to 90-nm COPII vesicles. Although there has been important progress in identifying receptors such as TANGO1 that guide the packing of PCs into COPII transport carriers (*2*–*4*), the growth promotion mechanism of such megacarriers is unknown, as is the nature of the timer that delays fission of the nascent carriers until they reach an adequate size.

Spondyloepiphyseal dysplasia tarda (SEDT) is an X-linked skeletal disorder characterized by short stature, a short trunk, and precocious osteoarthritis. SEDT is caused by mutations in the gene *SEDL* (*5*); the underlying defect is a derangement in chondrogenesis reflecting the inability of chondrocytes to properly secrete extracellular matrix components (*6*). Sedlin, the *SEDL* product, is a component of a highly conserved multisubunit complex, TRAPP, which functions at various steps in intracellular transport (*7*), but the role of Sedlin (also called TRAPPC2) in these processes remains unknown.

The observations that a defect in Sedlin leads to cartilage-restricted consequences, and that there are shared clinical signs between patients with some mutations of type II PC (PCII) (*8*, *9*) and Sedlin (*5*), prompted us to examine the impact of Sedlin knockdown (KD) (fig. S1) on trafficking of PCII in chondrocytes (*10*) and, in comparison, on trafficking of a reporter cargo, the temperature-sensitive variant of vesicular stomatitis virus G protein (ts045–VSV-G). The transport of PCII and VSV-G along the secretory pathway was synchronized by incubating cells at 40°C, resulting in reversible misfolding and ER retention of both cargoes, and then shifting the cells to 32°C to release the ER block (*11*). PCII transport was impaired by Sedlin depletion, with a marked inhibition of its ER exit (Fig. 1, A and B, and fig. S2A) and extracellular secretion (Fig. 1C). This impairment was partially rescued by expression of an RNA-resistant form of Sedlin (Fig. 1B). By contrast, transport of newly synthesized VSV-G was indistinguishable in Sedlin-depleted cells relative to control cells (Fig. 1, A and B, and fig. S2B). Sedlin KD did not appreciably affect total protein secretion (Fig. 1D). We extended our analysis to the transport of other cargoes, including type I PC (PCI), CD8α (Fig. 1E), albumin, and α1-antitrypsin. (Fig. 1F). PCI was the only cargo whose ER exit was affected by Sedlin depletion. All other cargoes examined exited the ER and reached the plasma membrane at apparently normal rates. Sedlin plays its role in PC trafficking as a TRAPP component, because a similar selective impairment of the ER exit of PC was induced by depleting the whole TRAPP by knockdown of

[1]Telethon Institute of Genetics and Medicine, Via Pietro Castellino 111, Naples 80131, Italy. [2]Consorzio Mario Negri Sud, Via Nazionale, Santa Maria Imbaro (Chieti) 66030, Italy. [3]Medical Genetics Unit, IRCCS Casa Sollievo della Sofferenza, 71013 San Giovanni Rotondo, Foggia, Italy. [4]Department of Cell and Developmental Biology, Centre de Regulacio Genomica, 08010 Barcelona, Spain. [5]Institució Catalana de Recerca i Estudis Avançats, Pg. Lluis Companys 23, 08010 Barcelona, Spain. [6]Department of Cell Biology and Anatomy, Rosalind Franklin University of Medicine and Science, North Chicago, IL 60064, USA.

*These authors contributed equally to this work.
†Present address: Division of Cell Biology, Netherlands Cancer Institute, Plesmanlaan 121, 1066 CX Amsterdam, Netherlands.
‡Present address: IFOM-IEO Campus, Via Adamello, 20139 Milan, Italy.
§Present address: Faculty of Life Sciences, University of Manchester, Manchester M13 9PT, UK.
||To whom correspondence should be addressed. E-mail: dematteis@tigem.it